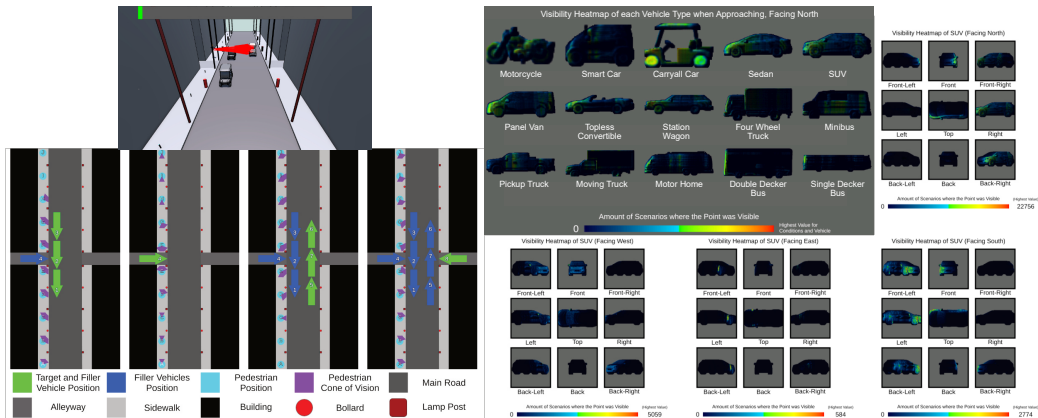


Graphical Abstract

Analytical Study on the Visibility of Potential Positions for External Human-Machine Interfaces

Jose Gonzalez-Belmonte, Jaerock Kwon



Highlights

Analytical Study on the Visibility of Potential Positions for External Human-Machine Interfaces

Jose Gonzalez-Belmonte, Jaerock Kwon

- Many papers have addressed the effectivity of External Human-Machine Interfaces (eHMIs), and positioning of the display is considered an important consideration.
- Despite this, little research is available on the best placement of eHMIs to maximize visibility. This paper focuses on finding the best positioning for eHMIs on approaching vehicles meant to be seen by pedestrians on the sidewalk.
- A 3D simulation software was developed using the Unity game engine. This software was used to find what points of the simulated vehicle are most often visible for the tested pedestrian positions.
- The simulation was repeated with fifteen different vehicles across three different distance ranges to ensure that the results were not only applicable to a single type or model of vehicle.
- It was found that the best position on the exterior of an approaching vehicle to maximize an eHMI's visibility were the front fenders and the headlights.
- The software developed for this work will provide a platform where similar studies can be systematically done in the future.

Analytical Study on the Visibility of Potential Positions for External Human-Machine Interfaces

Jose Gonzalez-Belmonte^a, Jaerock Kwon^a

^a*University of Michigan - Dearborn, 4901 Evergreen Rd, Dearborn, 48128, Michigan, United States of America*

Abstract

As we move towards a future of autonomous vehicles, questions regarding their method of communication have arisen. One of the common questions concerns the placement of the signaling used to communicate with pedestrians and road users, but little work has been published fully dedicated to exploring this. This paper uses a simulation made in the Unity game engine to record the visibility of fifteen different vehicles, specifically regarding the visibility of frontal elements by a pedestrian on the sidewalk. Variables include the vehicle position, number of vehicles on the road, and minimum and maximum distance of the recorded points. It was concluded that the areas of the vehicle most often seen by pedestrians on the sidewalk attempting to cross the road were the frontal fenders and the headlights, with the frontal wheels, frontal doors, bumper, and side mirrors are less visible alternatives. These findings are valuable in the future design of signaling for autonomous vehicles, in order to ensure pedestrians are able to see them on approaching vehicles. The software used provides a platform for similar works in the future to be conducted.

Keywords:

autonomous vehicles, eHMI, road safety, pedestrian safety

1. Introduction

In the field of Autonomous Vehicles (AVs), external human-machine interfaces (eHMIs) refer to methods of communication, such as screens or lights, that an AV can use to communicate with other road users. With traditional vehicles, drivers are able to use body language to communicate implicitly with pedestrians, but the introduction of AVs introduces a “social void” through

the removal of an attentive human driver who can handle ambiguous road interactions (de Winter and Dodou (2022)). EHMI were introduced as a solution to this problem, aiming to eliminate ambiguity and the necessity of inter-personal social cues by letting the AV outwardly explicitly express its intent to pedestrians.

Studies have been done previously regarding the effectiveness of eHMIs (de Clercq et al. (2019); Rodríguez Palmeiro et al. (2018); Alhawiti et al. (2024)) and the symbols they should use (de Winter and Dodou (2022)), but few studies have been conducted that are focused on determining the ideal position for these displays. Those available are limited in how data is collected and represented (Troel-Madec et al. (2019)), or concerned primarily with what position an observant pedestrian prefers (Guo et al. (2022)). Few studies address the question of varying vehicle types, meaning that the results may possibly not work with larger or smaller vehicle types.

As observers must be able to perceive an eHMI before making a decision based on its information, the lack of studies addressing the visibility of these elements is a gap in the knowledge necessary to set standards for this technology.

This study aims to expand on these results by introducing a data-capturing method with higher precision, and making use of a wider variety of scenarios and vehicles. The intent is to develop an open-source software capable of simulating the possible positions for a vehicle and produce a heatmap indicating what parts and areas of the vehicle were visible in the highest amount of scenarios, then determine general recommendations for eHMI placement based on the results from a variety of vehicle types and permutations.

2. Related Work

The effectiveness of eHMIs has been thoroughly investigated through experiments using virtual reality (de Clercq et al. (2019)), video-based eye tracking techniques (Guo et al. (2022)), the Wizard of Oz method (Rodríguez Palmeiro et al. (2018)), and outdoor experiments using real autonomous vehicles (Alhawiti et al. (2024)). In each of these examples the presence of an eHMI proved to increase response time and feelings of safety on pedestrians, however, each these experiments feature vastly different proposals of eHMIs, often varying in their positioning within the same study.

Studies on the positioning of eHMI are less common than those focused on their effectiveness. de Winter et al. (2020) had participants walk around

a busy parking lot with an eye tracking device, and found that most participants focus on the general parts of a vehicle that are affected by their movement, such as the wheels, the back, and the front of the vehicle. They also concluded that eHMIs must be visible from all angles due to the varied conditions in which pedestrians encounter them.

Guo et al. (2022) used an experiment where participants watched a video of a vehicle approaching from the right, while their gaze was being recorded, in order to determine what parts of the vehicle they paid attention to. The vehicles illustrated in this experiment may use one from six different eHMI proposals (flashing text, sweeping pedestrian icon, sweeping arrow, flashing smiley, flashing light band, and sweeping light bar) located in one of three different positions (grill, windshield, and roof). They could also have no eHMI at all, in which case only one yielded, while ten did not. The results determined the windshield to be the locations of the vehicle with the longest visual attention from participants, followed closely by the grill, but found little difference in the efficiency of an eHMI based on said location.

A similar experiment to the one done for the present paper is that of Troel-Madec et al. (2019), where a 3D simulation was created to measure what parts of the vehicle were visible most of the time, and hence which areas were best suited for the placement of eHMIs, from the perspective of pedestrians looking at an incoming vehicle from the sidewalk. For this, the team placed three 3D models of a sedan vehicle in a virtual space, forming an unmoving line on the side closest to the sidewalk, facing towards the camera. Each vehicle was then assigned a different primary color, with differences in the shading based on what part of the vehicle they were in: front, side, and back. A virtual camera then took a series photos from a predefined set of points on the sidewalk at varying heights. The pixels on the resulting images were analyzed, using the solid color of the vehicles to find what parts of the each vehicle were visible the most. The results pointed to the side of the vehicle to be the most consistently visible part of the vehicle, and the team used these results to develop a prototype for an eHMI that was positioned on the front doors and windshield rails.

These studies overall conclude that the specific location of an eHMI matters less than the fact said eHMI is visible to the observer (de Clercq et al. (2019)), and that pedestrians tend to fixate on parts of the vehicle such as the grill, the windshield, the wheels, and the general back and front, while the sides of the vehicle seem to be the general area most visible in most scenarios. While these results are promising, they lack granularity and are

always done with a single type of vehicle, coming from one specific direction.

The scope of this paper aims to find comparable results to those presented in Troel-Madec et al. (2019), and as such the configuration of the simulations are only concerned with the visibility of pedestrians looking at incoming vehicles.

3. Methodology

The following requirements must be met by the results in order to provide a specific visible area for the placement of eHMIs:

1. The resulting data must be as granular as possible, not just pointing at general parts of the car, but specifically highlighting what points of the vehicle were visible.
2. Since vehicles are capable of blocking the view of each other from pedestrians (e.g. when vehicles are in a line), the software must be able to calculate all possible scenarios where this may happen and simulate all of them.
3. Multiple vehicles of different sizes must be simulated to ensure the results are versatile and universal.
4. Vehicles may come from four possible directions, respective to the sidewalk: two perpendicular to it, and two parallel to it. The simulation must present cases where this can be explored.

A simulation software was created to achieve these goals. A simulation instance produced by it can be divided into a hierarchy made of five levels, each made up of the ones after:

1. A *Simulation Run* is the highest level, where the user provides the program with the parameters that it will use during the simulation. These include:
 - The driving direction of the road: right-hand or left-hand.
 - The type of vehicle used.
 - The set of *Camera Positions* that will be used to capture the information, along with the possible *Camera Directions* that may be used at each.
 - The positions that the *Target Vehicle* may occupy. This is the vehicle that is being measured, where the visibility of the camera is projected on.

- The positions that the *Filler Vehicles* may occupy. These are other vehicles, identical to the *Filler Vehicle* but without recording any data.
- The number of vehicles in the scenario, including the *Target Vehicle* and *Filler Vehicles*. There will always be one and only one *Target Vehicle* in any given simulation. There may never be more *Filler Vehicles* in the road than there are positions for it. Entering '1' will make it so no *Filler Vehicles* are ever present in the simulation.
- The minimum and maximum distance that a point on the *Target Vehicle* may be from the camera for it to be recorded.

Based on these parameters, the software will instantiate a *Target Vehicle* in the pre-made environment, calculate all possible permutations of the *Target Vehicle* and the *Filler Vehicles* in their possible positions, then cycle through each of these *Scenarios* using the specified settings.

2. A *Scenario* represents a combination of different placements on the road for the *Target Vehicle* and other *Filler Vehicles* on the road. Since we want to find the points of the *Target Vehicle* that are visible the most often, we want to cycle through all possible combinations of *Filler Vehicle* placements to simulate the ways in which other vehicles on the road may block the view of the pedestrian.
3. For each scenario, the camera will cycle through each of the *Camera Positions*. For this paper, these all correspond to positions where a pedestrian may be located on the left sidewalk.
4. For each *Camera Direction* available at each *Camera Position*, the camera executes a series of *Data Captures* at five different heights from the floor: 1m, 1.2m, 1.4m, 1.6m, and 1.8m.
5. To perform a *Data Capture*, the camera simulates a series of ray-casts in a grid pattern coming from the camera to replicate where it is observing the *Target Vehicle*. Each ray-cast starts at the minimum distance away from the camera, and ends at its maximum distance. Ray-casting allows us to find the intersection point between an origin point and a destination point, as well as the details of the first collider hit this way, such as what object it belongs to or what components are attached to that game object (Aversa (2022)).

A diagram showing the layout of the virtual environment used by the

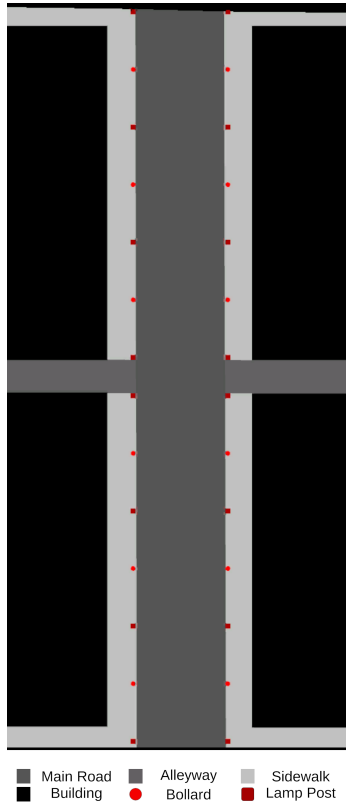


Figure 1: Top-Down View of the Virtual Street Layout.

simulation software can be seen in Fig. 1. A sample showing the software in action can be seen in Fig. 2.

The virtual environment for this simulation consists of a two-way street with alleyways intersecting it from the left and the right. The main road in this virtual intersection is 6.94m wide and 57.719m long; the alleyways are 2.604m wide; both sidewalks are 2.216m wide and 0.102m tall; the four cuboids that stand for buildings in this model are each 21.5m tall, and cover the space not occupied by the alleyways or the road.

The virtual sidewalk was also populated by static objects that serve as obstacles in the observer's view. There are two kinds of obstacles, each placed in alternate order on the sidewalk 4.5m from each other. Both sidewalks are mirrored.

- **Bollards:** Each a cylinder 0.305m in radius and 0.914m in height.

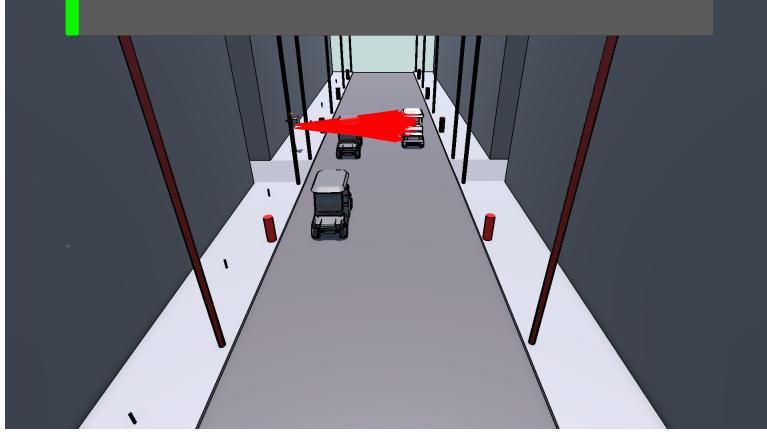


Figure 2: Screenshot of the simulation running. Red lines indicate the trajectory of the ray-casts that have hit the *Target Vehicle*.

No cylinder is placed in the space taken by an alleyway intersecting a sidewalk. All cylinders are positioned 0.063m away from the edge of the curb. There are a total of 12 bollards on the scene. Visible as red circles in Fig. 1.

- **Lamp Posts:** A series of tall cylinders representing lamp posts placed on the sidewalk, 0.161m from the edge. Each tall cylinder is 0.152m in radius and 9m in height. Six are placed on each sidewalk, 9m from each other. There are a total of 16 lamp posts on the scene. Visible as red squares in Fig. 1.

The vehicles to be used in this simulation had to be representative of the variety of vehicles that can be found on the road. The fifteen vehicles seen in Table 1 were selected, using the list of vehicle types outlined by the Federal Highway Administration as a base. All models were found and downloaded for free from the online website Sketchfab.com under the Creative Commons license. Each model, the vehicle type it corresponds to, and its closest real-life equivalent can be seen in Table 1, with notes providing additional context if the specific model was not specified.

Based on their dimensions, the vehicles selected were broken into four categories, based on their length and classification in Federal Highway Administration:

Category	Model	Modeler	Notes
Motorcycle	Honda Shadow RS 2010	[@Alex.Ka.] (2022)	
Smart Car	Smart Fortwo	[@beztao01] (2021)	
Carryall Car	N/A	[@maxdragon] (2021)	Described as a "Golf Cart"
Sedan	N/A	Daniel Zhabotinsky [@DanielZhabotinsky] (2020b)	Described as "Based on asian design features of last decade [2010s]."
SUV	Ford Edge 2006	[@fishermans] (2024)	
Panel Van	D3S MB Vito Panel Van (W447) '15	[@danzzzeg] (2017)	
Topless Convertible	N/A	[Brian N.] (2007)	Chrysler Sebring Convertible. Specific model not specified. Page removed.
Station Wagon	80s Lincoln Zephyr Mercury	Daniel Zhabotinsky [@DanielZhabotinsky] (2020a)	
Minibus	Peugeot J5	[@boitaloran] (2022)	
Four wheel Truck	N/A	Daniel Zhabotinsky [@DanielZhabotinsky] (2020c)	Described as a generic Japanese-made small-cabin commercial truck from the 90s.
Pickup Truck	2015 Ford F150 King Ranch Edition	David Holiday [@David.Holiday] (2021)	
Moving Truck	N/A	Daniel Zhabotinsky [@DanielZhabotinsky] (2021)	Described as a generic Japanese-made 2-door pickup-cabin box truck.
Motor home	N/A	Lion Sharp [lionsharp] (2013)	Modified GMC Motorhome
Double Decker Bus	N/A	[@businessyuen] (2020)	Described as a "Hong Kong Bus", corresponding to a Volvo B8L
Single Decker Bus	N/A	[@own.guest] (2021)	

Table 1: List of vehicles used in the simulations.

- **Small (S):** Vehicles under Class 1, and vehicles of Class 2 less than 4m in length (Fig. 3(a)).
- **Medium (M):** Vehicles under Class 2 and Class 3 between 4m and 6m in length (Fig. 3(b)).
- **Large (L):** Vehicles under Class 3, Class 4, and Class 5 between 6m and 8m in length (Fig. 3(c)).
- **Extra Large (XL):** Vehicles under Class 4, Class 5, and Class 6 longer than 8m (Fig. 3(d)).

Since all vehicle models were made by a third-party, it is important to consider the dimensions of the virtual vehicles with the real counterpart of those vehicles to ensure accuracy. Adjustments were made to the size of the vehicles to more closely resemble their real-life equivalents. A comparison of both can be seen in Table 2.

The model has eight possible positions for vehicles.

- **On the Road:** Three of the positions are on the left side (Fig. 4(a to d)(1 to 3)) and three on the right side (Fig. 4(a to d)(5 to 7)).

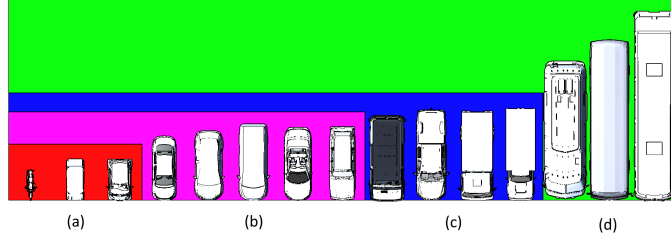


Figure 3: Top-Down View of the fifteen vehicles used in the simulations. Color denotes the category of each vehicle: (a) Small (b) Medium (c) Large (d) Extra Large

Vehicles in each set of positions face in the same direction, forming a line. For this work, the American driving direction was used (right side), so vehicles on the west side of the image drive towards the south, while those on the east side drive northward.

- **Exiting Alleyway:** Two of the positions place the vehicle intersecting with the sidewalk, facing towards the road (Fig. 4(a to d)(4,8)). This emulates vehicles turning into the road, as well as vehicles driving across the intersection.

The front of the spawned vehicles are aligned with the pivot point they are placed in. To ensure that vehicles wouldn't overlap, the specific position of each of the six pivots on the main road varies depending on the size of the vehicle being evaluated. Table 3 shows the distance between pivots for each size category, while Fig. 4 illustrates them.

This means that the space between the front of a vehicle, and the back of the one its facing will vary between vehicles. Table 4 shows what this distance is for all fifteen vehicles used in the simulation.

At any given time, one and only one of the vehicles currently in the environment may record the points where it is being observed by the recording camera, this is considered the *Target Vehicle*. In each *Scenario*, the rest of the spaces that are occupied by vehicles are all filled with *Filler Vehicles* that use the same model as the *Target Vehicle*, but do not record any data.

Since the position of a vehicle on the road will vary regularly, and hence parts of said vehicle may be blocked by another vehicle, the simulation generates all possible combinations of *Target Vehicle* and *Filler Vehicle* positions, based on whether a position is occupied by the target vehicle, a filler vehicle, or no vehicle. At the start of a *Simulation Run*, the user also decides

Vehicle Size Category	Real Life Dimensions (m)			Dimensions in Simulation (m)		
	H	W	L	H	W	L
Motorcycle	1.13	0.92	2.51	1.15	0.86	2.14
Smart Car	1.54	1.56	2.70	1.71	1.88	2.78
Carryall Car	-	-	-	1.78	1.22	2.79
Sedan	-	-	-	1.44	1.71	4.35
SUV	1.70	1.93	4.72	1.63	2.08	4.71
Panel Van	1.90	1.93	4.90	1.91	1.91	4.89
Topless Convertible	-	-	-	1.31	1.93	4.94
Station Wagon	1.38	1.80	4.97	1.36	1.83	4.98
Four wheel Truck	2.92	1.97	4.77	2.61	2.84	6.02
Minibus	2.42	1.97	5.49	2.46	2.62	5.81
Pickup Truck	2.00	2.03	6.18	1.86	2.35	6.03
Moving Truck	-	-	-	2.46	2.09	6.25
Motor home	-	-	-	3.21	3.02	9.12
Double Decker Bus	-	-	-	4.79	2.77	11.10
Single Decker Bus	-	-	-	3.12	3.17	12.80

Table 2: Dimensions of the virtual vehicles and their real-life equivalents, in meters.

what positions the *Active Vehicle* may be in, as well as which ones the *Filler Vehicles* may occupy, and how many *Filler Vehicles* there may be on the *Scenarios* tested.

The simulation has a single camera that, through a series of *Data Captures*, records what parts of the *Target Vehicle* are being observed. During the simulation, the camera cycles through a list of *Camera Positions*, their possible *Camera Directions*, and their possible heights. A visual example of this process can be seen in Fig. 2.

When the camera is at a specific *Camera Position*, it must take a *Data Capture* for each possible facing that a road user may have in that position. To replicate this, each point has a list of valid facing directions that the camera cycles through. During setup, each *Camera Position* has eight directions available, each corresponding to a cardinal direction relative to the overhead camera, as seen in Fig. 2: North, North-East, East, South-East,

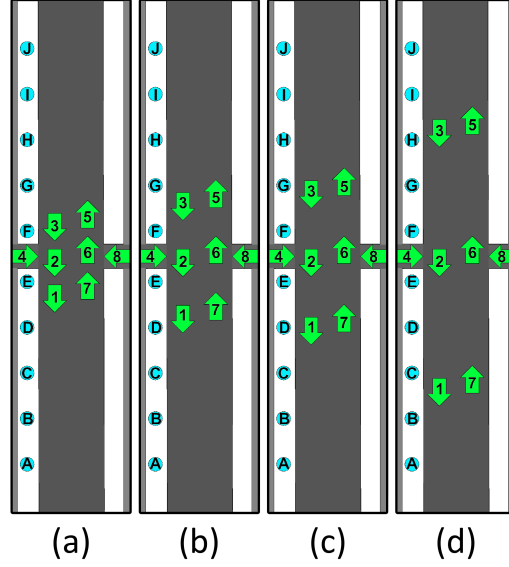


Figure 4: Diagram illustrating the ten possible sidewalk camera positions, and the eight possible vehicle positions, based on the size categories of the target vehicle. (a) Small vehicles (b) Medium vehicles (c) Large vehicles (d) Extra large vehicles.

South, South-West, West, North-West.

Since our roads are shared with people of varied heights, the camera needs to get *Data Captures* from different heights. For each *Camera Direction*, the camera cycles through five camera heights, based on the same five used in Troel-Madec et al. (2019): 1m, 1.2m, 1.4m, 1.6m, and 1.8m. These values are not adjustable.

Vehicle Category	Distance (m)
Small	3.792
Medium	5.970
Large	7.240
Extra Large	13.730

Table 3: Distance between each vehicle position on the road

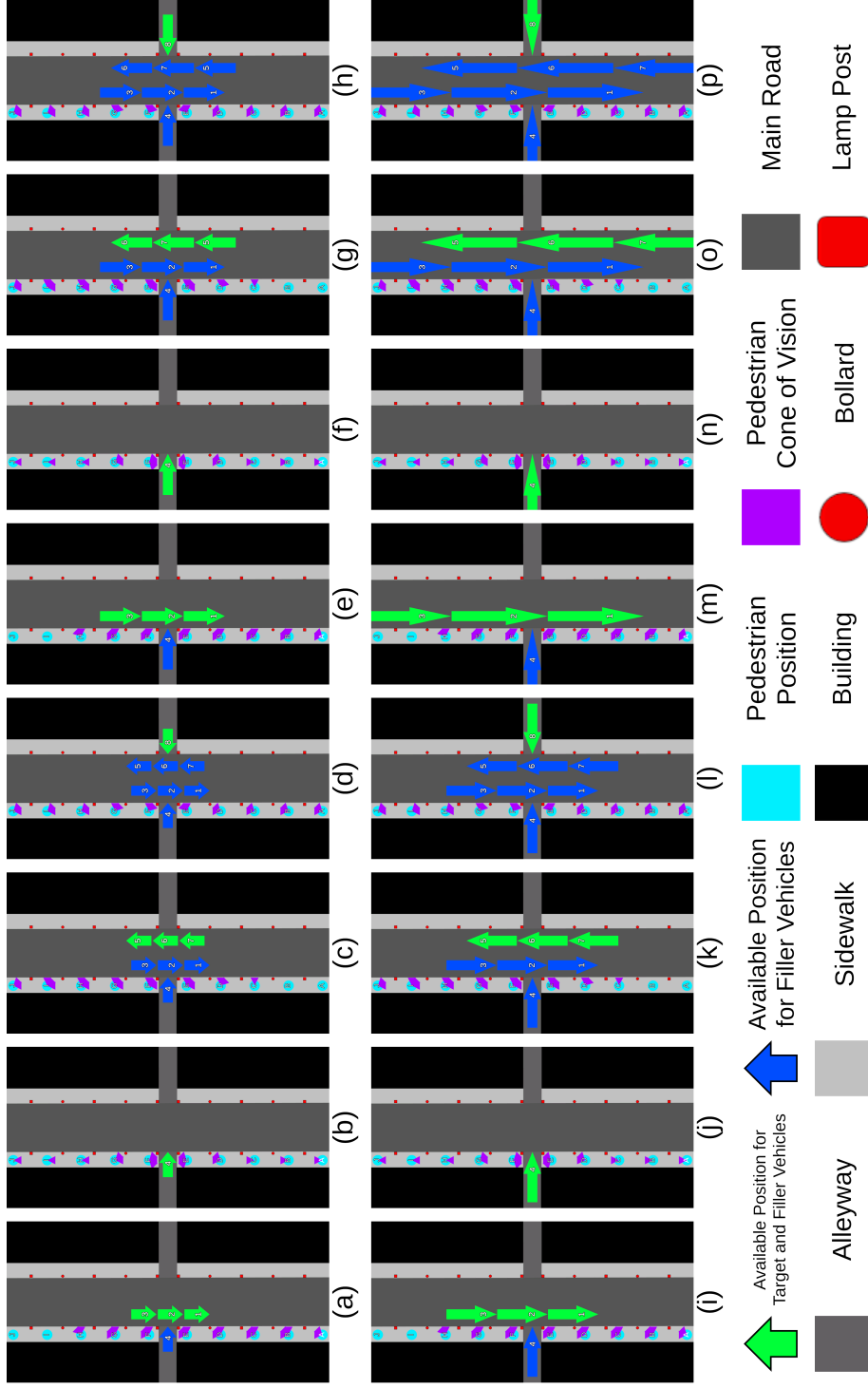
Category	Vehicle Type	Bumped-to-Bumper Distance (m)	Vehicle Length (m)
Small	Motorcycle	1.65	2.14
Small	Smart Car	1.01	2.78
Small	Carryall Car	1.00	2.79
Medium	Sedan	1.62	4.35
Medium	SUV	1.26	4.71
Medium	Panel Van	1.08	4.89
Medium	Topless Convertible	1.03	4.94
Medium	Station Wagon	0.99	4.98
Large	Four wheel Truck	1.22	6.02
Large	Minibus	1.43	5.81
Large	Pickup Truck	1.21	6.03
Large	Moving Truck	0.99	6.25
Extra Large	Motor home	4.61	9.12
Extra Large	Double Decker Bus	2.63	11.10
Extra Large	Single Decker Bus	0.93	12.80

Table 4: Distance between each vehicle when forming a line on the same lane.

4. Experiment Setup

The software developed for the simulation was made using the Unity game engine, version 2022.3.28f1, and C#. Blender 4.2 was used to model the street and re-pivot the vehicles. Most of the data capture process was done using Unity’s built in physics system, specifically it’s ray-casting functionality.

Fig. 5 illustrates the configuration of all positions that *Target Vehicles* and *Filler Vehicles* occupied for this experiment, depending on their type.



Since the amount of filler vehicles on the road will influence how much of the *Target Vehicle* is visible, multiple *Simulation Runs* were done varying the number of *Filler Vehicles* on the road.

- The total amount of vehicle may be between 1 and 4 for scenarios where the *Target Vehicle* is on the road closest to the sidewalk. This is because visibility in that case may only be affected by *Filler Vehicles* placed on the sidewalk (Fig. 5 (a, e, j, n)(4)) or in front of it (Fig. 5 (a, e, j, n)(1,2,3)).
- The total amount of vehicles is always 1 when the *Target Vehicle* is located on the west alleyway (Fig. 5 (b, f, j, n)), since *Filler Vehicles* on any other position will never block view from it.
- The total amount of vehicles may be between 1 and 7 when the *Filler Vehicle* is located on the right-hand side of the road (Fig. 5(c, g, k, o)(1 to 4)), since it may be blocked by other vehicles in those positions, as well as vehicles on the left side (Fig. 5 (c, g, k, o)(5,6,7)).
- The total amount of vehicles may be between 1 and 8 when the *Target Vehicle* is positioned on the east alleyway (Fig. 5 (d, h, l, p)(1 to 7)), since it can be blocked by any other vehicle on the road.

During setup, each *Camera Position* has a total of ten possible positions that it may cycle through on the sidewalk (Fig. 4(a,b,c,d)(A to J), Fig. 5(a to p)(A to J)).

For the simulations in this paper, camera positions were chosen based on four possible vehicle facings, minimizing cases where the pedestrian would not be able to see the front of the vehicle:

- If the *Target Vehicle* is going southwards, *Data Captures* will only happen towards the East, Northeast, and North (Fig. 5 (a, e, i, m)).
- If the *Target Vehicle* is coming out of the left alleyway, going eastwards, *Data Captures* will only happen towards the North, Northeast, South, and Southeast (Fig. 5 (b, f, j, n)).
- If the *Target Vehicle* is going northwards, *Data Captures* will only happen towards the East, Southeast, and South (Fig. 5 (c, g, k, o)).

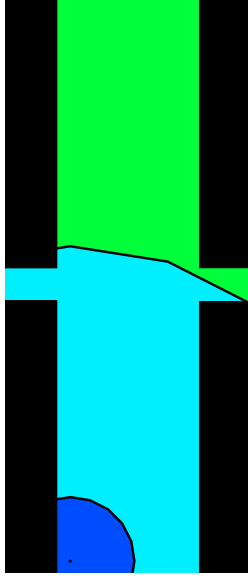


Figure 6: Visualization of the three ranges used for *Data Capturing* for this experiment: Blue: 0m to 5m; Cyan: 5m to 25m; Green: 25m to 75m.

- If the *Target Vehicle* is coming out of the right alleyway, going westwards, *Data Captures* will only happen towards the North, Northeast, South, and Southeast (Fig. 5 (d, g, l, p)).

For this experiment, in order to produce data on how the distance between the *Target Vehicle* and the camera may affect the visibility of certain elements, each set of nineteen scenarios were was three times with different minimum and maximum distances for the *Data Capture*: 0m to 5m, 5m to 25m, and 25m to 75m. Fig. 6 puts these values into scale within the environment of the simulation.

The system for recording data is mainly controlled by three scripts: The *Heatmap Sender*, placed on the camera; the *Heatmap Receiver*, placed on the *Target Vehicle*; and the *Heatmap Display* placed on the *Target Vehicle*.

At the start of the simulation, the *Heatmap Display* simplifies the mesh of the vehicle into a grid of *Grid Points*, where each is a structure containing the internal tridimensional coordinates of that point on the grid. Each *Grid Point* also holds a long integer value representing how many times that point has been hit by the *Heatmap Sender*. All points in the grid are in contact with the mesh of the vehicle. This system is used to round the information

received for later display.

In each *Data Capture*, the camera casts a total of 14 400 straight rays in a 160x90 grid pattern. These rays are cast in the facing direction of the camera using Unity’s *ScreenPointToRay* function, which adjusts for the camera’s 60 degree field of view.

When one of the rays cast by the *Heatmap Sender* hits the *Target Vehicle*, the tridimensional point of contact is recorded internally in local coordinates by the *Heatmap Receiver*. At the end of each *Data Capture*, once all rays have been cast by the *Heatmap Sender*, the *Heatmap Display* rounds each of the points recorded to the nearest equivalent *Grid Point* (if applicable). Every time a point on the *Heatmap Receiver* is rounded to a *Grid Point*, the value associated with said *Grid Point* is increased by one.

To prevent proximity bias, produced by multiple local coordinates being rounded to the same *Grid Point* in the same *Data Capture*, *Grid Points* may only increase their value once per *Data Capture*.

Once the simulation has run through all *Scenarios*, the points stored and their associated values are serialized into a JavaScript Object Notation (JSON) file that can be read by the software. This represents the end of the simulation.

In a separate Unity scene, the software is able to load the JSON files it has produced. The user may select one of the fifteen vehicles listed above (Table 1) and the JSON files they would like to see displayed. The software will then instantiate a copy of the selected vehicle and add the data from the JSON files to that vehicle’s Heatmap Display through an additive process. The result is then presented to the user so they can inspect it and take virtual photographs of the vehicle facing nine of its possible angles: front, front-right corner, right flank, back-right corner, back, front-left corner, left flank, front-left corner, and directly from above.

We refer to the images produced this way during our analysis of the results. Fig. 7 provides a visual aid identifying and the language consistently used to refer to each during the data analysis part of this paper.

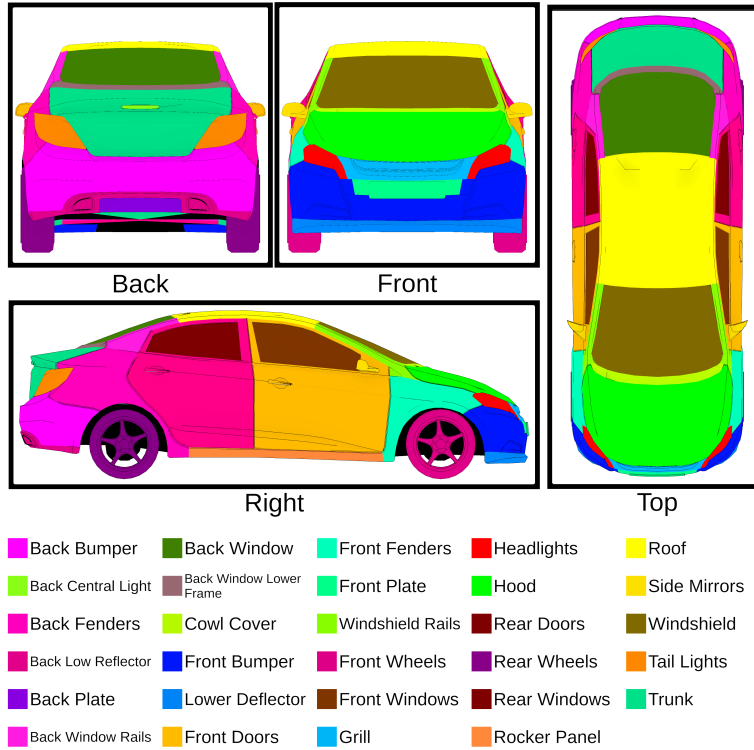


Figure 7: Illustration of the different exterior parts of a sedan, and the terminology used to refer to each.

The simulation was run a total of nineteen times for each vehicle, producing a total of 855 output files.

5. Results

A total of 855 separate simulations were run in order to produce data that could represent the visibility of all fifteen selected vehicles under the three different ranges. Since the number of *Scenarios* varies depending on the position of the vehicle, the addition of all files corresponding to a given vehicle type produces results biased towards scenarios where the vehicle was on the right side of the street, this is because the higher amount of *Filler Vehicle* positions means there are more permutations to be tested, which leads to a higher amount of opportunities for a point to be seen multiple times.

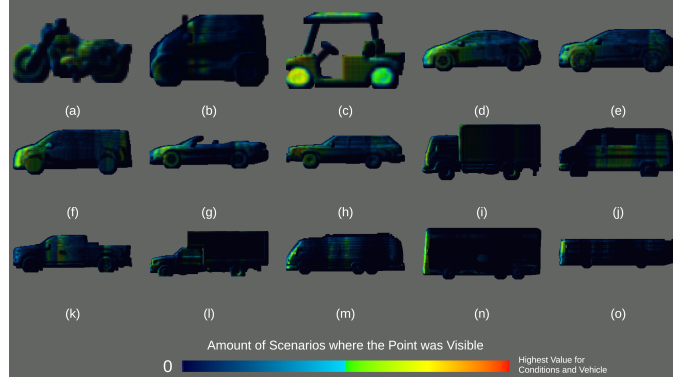


Figure 8: Comparison of the right side of the heatmap of all vehicle types that is produced when these are driving North.

(a) Motorcycle (b) Smart Car (c) Carryall Car (d) Sedan (e) SUV (f) Panel Van (g) Topless Convertible (h) Station Wagon (i) Four Wheel Truck (j) Minibus (k) Pickup Truck (l) Moving Truck (m) Motor Home (n) Double Decker Bus (o) Single Decker Bus

Because of this, results were divided into four categories: facing South, facing East, facing North, and facing West. A picture was produced for each, showing the resulting heat map colored according to how many times they were recorded during the simulation for said vehicle. Since each *Grid Point* can only be recorded once per *Data Capture*, this color also represents the amount of circumstances under which a specific *Grid Point* was recorded. A comparison of all vehicle heatmaps can be seen in Fig. 8.

For this publication, only the images depicting the resulting heatmap of the SUV model are included (Fig. 9) , however all produced data was analyzed as well.

Additionally, in order to discover the impact of distance on the visibility of the vehicle, Fig. 10 shows the heatmap of the SUV vehicle at each of the four facing categories (Facing South (Fig. 10(a to c)), Facing East (Fig. 10(d to f)), Facing North (Fig. 10(g to i)), Facing West (Fig. 10(j to l))), and each of the three distance thresholds (0m to 5m (Fig. 10(a, d, g, j)), 5m to 25m (Fig. 10(b, e, h, k)), 25m to 75m (Fig. 10(c,f,i,l))

5.1. Heatmap Comparison

With the heatmaps produced, the need existed to identify individual elements on the vehicle exterior in order to provide general recommendations for eHMI placement. Fig. 7 identifies each part on the exterior of the vehicle used for this experiment.

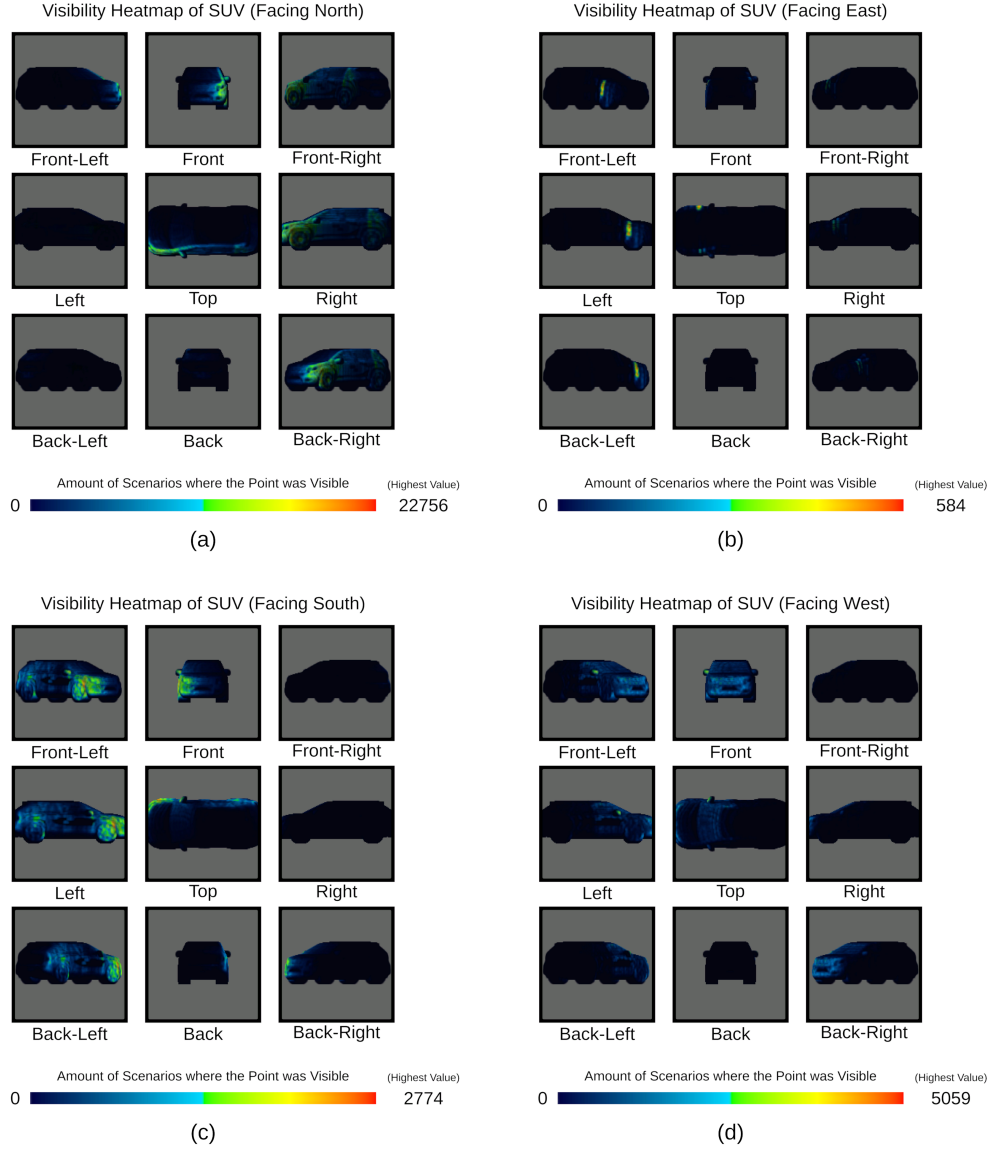


Figure 9: Results showing how many times a *Grid Point* was recorded, across all scenarios where the vehicle was a SUV driving: (a) North, on the right side of the virtual environment; (b) East, out of the alleyway on the left side of the virtual environment; (c) South, on the left side of the virtual environment; (d) West, out of the alleyway on the right side of the virtual environment.

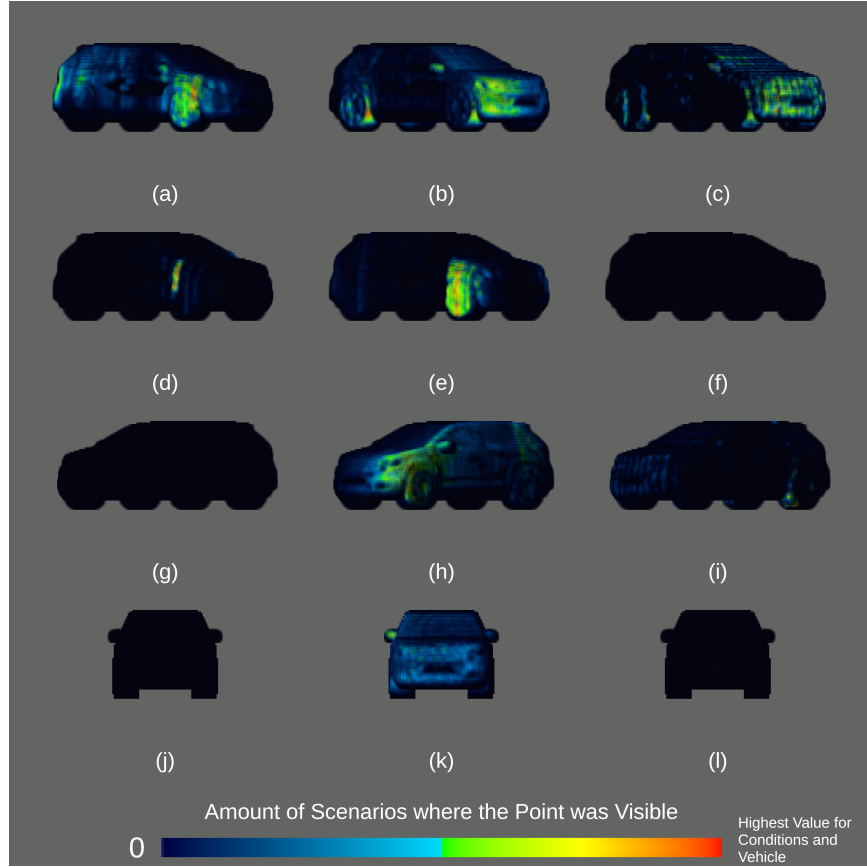


Figure 10: Results showing the heatmap of the SUV at each facing direction, when the observer is at each distance threshold.

The sixty heatmaps produced (one for each combination of vehicle and facing direction) were analyzed, comparing them against the identified exterior elements in order to produce Table 5, where a facing direction was annotated each time at least one *Grid Point* on that element shows coloration indicating it was recorded in at least 50% of the tested cases for that combination of conditions.

Based on these observations, the six element most often visible in the analyzed heatmaps, in descending order, are:

1. The front fenders (76.67%)
2. The headlights (63.33%)
3. The front wheels (61.67%)

Vehicle Type	The element is visible when the vehicle is facing in the directions...									
	Back Bumper	Back Central Light	Back Fenders	Back Low Reflector	Back Plate	Back Window Rails	Back Window	Back Window Lower Frame	Cowl Cover	Front Bumper
Carryall Car			N S			W			*	*
Double decker bus			S				S		S W	N S W
Four wheel Truck							*	*		N S
Minibus			N S			S	N			N
Motorcycle		*	N S	*		*	*	*	*	*
Motor home			S						N	N S W
Moving Truck			S			*	*	*		N S W
Panel Van			N S			N				N S W
Pickup Truck			S	S		S				S
Sedan			N				W		N W	N S W
Single decker bus									*	N S W
Smart Car			W			W	*	*	S	N W
Station Wagon			S	S		N	S			N S W
SUV			N S						E	S W
Topless Convertible			N S			*	*			S W
Count	0	0	19	2	0	6	4	0	7	31
Percentage	0.00%	0.00%	31.67%	3.33%	0.00%	10.00%	6.67%	0.00%	11.67%	51.67%

Vehicle Type	The element is visible when the vehicle is facing in the directions...									
	Lower Deflector	Front Doors	Front Fenders	Front Plate	Windshield Rails	Front Wheels	Front Windows	Grill	Headlight	Hood
Carryall Car		N S E W	N S		S W	N S W	*	*	N S	N W
Double decker bus	N W	S E	N S W		N S	S W	S W	N W	N S W	*
Four wheel Truck	N S E W	E	N S		N	N S E W	E	S	N S W	
Minibus	E	N S E W	N			E				N
Motorcycle	*	*	N S W	*	*	N S E W	*	*	N S W	*
Motor home	N S E W	N S	N S E W		N	W	S W	N S	N S W	W
Moving Truck	N S	N E	N S E W			N S E	N	S	N S W	E
Panel Van	N	N S	N S E		N E W	N S E	N	N W	N S	N
Pickup Truck	S	N	N S E		N	S E	N	S	N S	
Sedan	N S W	N S E W	N S E W	W	N S E W	N S E	N W	W	N S W	E W
Single decker bus	N S W	S E W	N S W		N S		S	S W	N S W	*
Smart Car	W	N S E	N S W		S E	N W	N S E	W	N W	S W
Station Wagon	S W	N S	N S E W	W	N S W	N W	W	N W	N S W	E
SUV	S W	N S	N S E W		N E	N E		S W	N S W	S W
Topless Convertible	S	S W	N S E		N	N S E	*		N S W	S W
Count	27	34	46	2	24	37	15	17	38	15
Percentage	45.00%	56.67%	76.67%	3.33%	40.00%	61.67%	25.00%	28.33%	63.33%	25.00%

Vehicle Type	The element is visible when the vehicle is facing in the directions...								
	Rear Doors	Rear Wheels	Rear Windows	Rocker Pannel	Roof	Side Mirrors	Windshield	Tail Lights	Trunk
Carryall Car	*	N			N E	*	N S W		
Double decker bus	*		S	N	W	N W	N S W		
Four wheel Truck	*	N S		S		N	S		
Minibus	N S	N	N	S		W			
Motorcycle	*	N	*	N	*	N S E W	*		*
Motor home	*	S		N	W	N S W	N W		
Moving Truck	*	N S	*	N	N				
Panel Van	N	N	N			N S W			
Pickup Truck	N S	N S		N		N S W			
Sedan	S W	N	N W	N W	N W	N S E W	W		
Single decker bus	*				N W	N	N S W		
Smart Car	*	W	W			S			
Station Wagon			N		N W	W	S W		
SUV	N S	N S	N		W	N S W			
Topless Convertible			*		*	W			
Count	9	15	8	9	12	31	15	0	0
Percentage	15.00%	25.00%	13.33%	15.00%	20.00%	51.67%	25.00%	0.00%	0.00%

Table 5: A recounting of what elements from Fig. 7 are visible, on average, based on the direction the vehicle was facing at that time, where N relates to Fig. 5(c,g,i,o), S to 5(a,e,i,m), E to 5(b,f,j,n), and W to 5(d,h,l,n). (*) indicates when a vehicle did not possess a certain element.

4. The front doors (56.67%)
5. The front bumper and the side mirrors (tied at 51.67%)

Noticeably, the windshield was only visible in 25% of the heatmaps, likely due to vehicles in front blocking the view from the pedestrian angles in most cases. Its rails, concluded to be of high interest for pedestrians in Bazilinsky et al. (2019) and of high visibility in Troel-Madec et al. (2019), rank above most of the elements at 40.00%.

5.2. *Effects of Distance*

As seen in Fig. 10, the visibility of the vehicle *Grid Points* was low to none whenever the *Target Vehicle* was anywhere but driving South, on the lane closest to the sidewalk. In the case where distance did reveal different parts of the vehicle being visible, the front fender and the headlights were the most consistently visible parts (Fig. 8(a, b)).

5.3. *Effects of Vehicle Position*

The position of the vehicle plays an important role in determining visibility:

- The headlights and the front bumper are not visible in any of the scenarios where the vehicle was positioned intersecting with the pedestrian sidewalk, and the side mirrors are rarely visible (5(b,f,j,n)).
- The front wheels and the front doors are not as visible when the vehicle is intersecting the sidewalk opposite to the pedestrian's (5(d,h,l,p)).

5.4. *Parts Visible Most Often*

Based on the data observed, the most visible area on the vehicle exterior, generally across all vehicle types, and regardless of distance, are the front fenders, followed by the headlights.

6. Future Work

This paper aims to generate knowledge on the general visibility of different parts of the vehicles tested. The results represent those obtained under very specific circumstances, and more specific patterns may arise if changes are made to it.

Some future iterations of this experiment may use different vehicles, find data for left-hand driving, find the visibility heat map of vehicles in respect to other drivers, focus on the back of the vehicles, or add different obstacles such as traffic signs and parked vehicles.

Different layouts could also be tested, making changes to the currently used one such as widening the sidewalk, adding biking lane between the vehicles and the sidewalk, increasing the amount of lanes, adding a traffic light intersection, et cetera.

Finally, a limitation of the additive process used to produce visual results from the data is a bias towards data with higher values. While a weighting system is already implemented, it was not used in the generation of Fig. 9.

7. Conclusion

In this paper, we used a virtual simulation to determine the most visible parts of fifteen different incoming vehicles of drastically different shapes and sizes, when placed at multiple points in a two-way two-lane right-driving street with sidewalks. The results point to the frontal fenders and the headlights as the best placement for eHMIs communicating the intent of an incoming vehicle, with the front wheels, front doors, front bumper, and side mirrors as less visible alternatives.

While not particularly concurrent with the results and observations by Troel-Madec et al. (2019), it correlates with already-existing forms of signaling in modern vehicles. Additional testing might prove useful to better understand and contextualize these findings, but the data revealed in this experiment is valuable to design better forms of signaling in our modern roads that can be seen by their intended audience, especially as we steadily keep progressing to a future where autonomous vehicles roam our cities.

8. Declaration of Competing Interest

The author of this paper declares that they have no known competing financial interests or personal relationships that could have appeared to influence the work reported in this paper.

References

[@Alex.Ka.], 2022. Honda Shadow RS 2010. URL: <https://sketchfab.com/models/2e7cf7bc195044f4a0f60c04581e2691/embed?autostart=1>.

- Alhawiti, A., Kwigizile, V., Oh, J.S., Asher, Z.D., Hakimi, O., Aljohani, S., Ayantayo, S., 2024. The Effectiveness of eHMI Displays on Pedestrian–Autonomous Vehicle Interaction in Mixed-Traffic Environments. *Sensors* (Basel, Switzerland) 24, 5018. URL: <https://www.ncbi.nlm.nih.gov/pmc/articles/PMC11314639/>, doi:10.3390/s24155018.
- Aversa, D., 2022. Unity artificial intelligence programming : Add powerful, believable, and fun AI entities in your game with the power of Unity. Fifth edition ed., Packt Publishing, Birminham, UK.
- Bazilinskyy, P., Dodou, D., de Winter, J., 2019. Survey on eHMI concepts: The effect of text, color, and perspective. *Transportation Research Part F: Traffic Psychology and Behaviour* 67, 175–194. URL: <https://www.sciencedirect.com/science/article/pii/S1369847819302293>, doi:10.1016/j.trf.2019.10.013.
- [@beztao01], 2021. Smart By Material. URL: <https://sketchfab.com/models/27a7f393d3134e90b30d03bc6805cfb1/>.
- [@boitaloran], 2022. Peugeot J5 Minibus. URL: <https://sketchfab.com/models/55d72c5dd507464ca2fe26f782f8c04e/>.
- [Brian N.], 2007. Chrysler Sebring Convertible. URL: <https://sketchfab.com/3d-models/chrysler-sebring-convertible-dac8529f24754bbd936173cbe8da92b1>.
- [@businessyuen], 2020. Bus. URL: <https://sketchfab.com/models/cc159e95590b49999c6e08793eb0a76a/>.
- de Clercq, K., Dietrich, A., Núñez Velasco, J.P., de Winter, J., Happee, R., 2019. External Human-Machine Interfaces on Automated Vehicles: Effects on Pedestrian Crossing Decisions. *Human Factors* 61, 1353–1370. URL: <https://journals.sagepub.com/doi/10.1177/0018720819836343>, doi:10.1177/0018720819836343.
- Daniel Zhabotinsky [@DanielZhabotinsky], 2020a. American 80s Station Wagon - Low poly model. URL: <https://sketchfab.com/models/680e4ad1090f4e738bbd46e618f3a01f/>.

- Daniel Zhabotinsky [@DanielZhabotinsky], 2020b. Generic sedan 2010. URL: <https://sketchfab.com/models/7fd6e15785fa4aa9bfd6e31eb7c97ba6/>.
- Daniel Zhabotinsky [@DanielZhabotinsky], 2020c. Light Box Truck - Low poly model. URL: <https://sketchfab.com/models/cbc508a5ad424d79b2f2c8a3de7e1cd3/>.
- Daniel Zhabotinsky [@DanielZhabotinsky], 2021. '90 Light Commercial Truck - Low poly model. URL: <https://sketchfab.com/models/663a0953c038434a918cb85725c88ffa/>.
- [@danzzeg], 2017. D3S MB Vito Panel Van (W447) '15. URL: <https://sketchfab.com/models/98d85b403ba0426f84636b575319e4f7/>.
- David Holiday [@David_Holiday], 2021. 2015 Ford F150 King Ranch Edition. URL: <https://sketchfab.com/models/79ebd5caaf414ab08debc36157dbc878/>.
- Federal Highway Administration, . Office of Highway Policy Information - Policy | Federal Highway Administration. URL: https://www.fhwa.dot.gov/policyinformation/tmguid/tmg_2013/vehicle-types.cfm.
- [@fishermans], 2024. Ford Edge 2006 lowpoly for 3D-printing. URL: <https://sketchfab.com/models/dec7fe5f75874a9cb913e8e54dcd4954/>.
- Guo, F., Lyu, W., Ren, Z., Li, M., Liu, Z., 2022. A Video-Based, Eye-Tracking Study to Investigate the Effect of eHMI Modalities and Locations on Pedestrian–Automated Vehicle Interaction. Sustainability 14, 5633. URL: <https://www.mdpi.com/2071-1050/14/9/5633>, doi:10.3390/su14095633. number: 9 Publisher: Multidisciplinary Digital Publishing Institute.
- Lion Sharp [@lionsharp], 2013. FREE GMC Motorhome reimaged low poly. URL: <https://sketchfab.com/models/6hiH0iyDqXqtdD9wbqSbyLLhK mz/>.
- [@maxdragon], 2021. area 9 golf cart. URL: <https://sketchfab.com/models/5fd13a5303af4f3bbba993dad35f788/>.

- [@own.guest], 2021. Generic Town Bus. URL: <https://sketchfab.com/models/14fe03d792914d51b6c6250b393c44fd/>.
- Rodríguez Palmeiro, A., van der Kint, S., Vissers, L., Farah, H., de Winter, J.C.F., Hagenzieker, M., 2018. Interaction between pedestrians and automated vehicles: A Wizard of Oz experiment. *Transportation Research Part F: Traffic Psychology and Behaviour* 58, 1005–1020. URL: <https://www.sciencedirect.com/science/article/pii/S1369847817305715>, doi:10.1016/j.trf.2018.07.020.
- Troel-Madec, M., Boissieux, L., Borkowski, S., Vaufreydaz, D., Alaimo, J., Chatagnon, S., Spalanzani, A., 2019. eHMI positioning for autonomous vehicle/pedestrians interaction, in: Adjunct Proceedings of the 31st Conference on l’Interaction Homme-Machine, Association for Computing Machinery, Grenoble, France. pp. 1–8. URL: <https://hal.science/hal-02388847>, doi:10.1145/3366551.3370340.
- de Winter, J., Bazilinsky, P., Wesdorp, D., de Vlam, V., Hopmans, B., Visscher, J., Dodou, D., 2020. How do pedestrians distribute their visual attention when walking through a parking garage? An eye-tracking study. *Ergonomics* 64, 793–805. URL: <https://www.tandfonline.com/doi/epdf/10.1080/00140139.2020.1862310?src=getftr>.
- de Winter, J., Dodou, D., 2022. External human–machine interfaces: Gimick or necessity? *Transportation Research Interdisciplinary Perspectives* 15, 100643. URL: <https://www.sciencedirect.com/science/article/pii/S2590198222001051>, doi:10.1016/j.trip.2022.100643.